| | |
|---|---|
| Title | Strain effects and thickness dependence of ferroelectric properties in epitaxial BiFeO3 thin films |
| Author(s) | Ma, Hua; Chen, Lang; Wang, Junling; Ma, Jan; Boey, Freddy Yin Chiang |
| Citation | Ma, H., Chen, L., Wang, J., Ma, J., & Boey, F. (2008). Strain effects and thickness dependence of ferroelectric properties in epitaxial BiFeO3 thin films. Applied Physics Letters, 92. |
| Date | 2008 |
| URL | http://hdl.handle.net/10220/6927 |
| Rights | © 2008 American Institute of Physics. This paper was published in Applied Physics Letters and is made available as an electronic reprint (preprint) with permission of American Institute of Physics. The paper can be found at the following DOI: http://dx.doi.org/10.1063/1.2920192. One print or electronic copy may be made for personal use only. Systematic or multiple reproduction, distribution to multiple locations via electronic or other means, duplication of any material in this paper for a fee or for commercial purposes, or modification of the content of the paper is prohibited and is subject to penalties under law. |

# Strain effects and thickness dependence of ferroelectric properties in epitaxial $BiFeO_3$ thin films

Hua Ma, Lang Chen,[a] Junling Wang, J. Ma, and F. Boey
*School of Material Science and Engineering, Nanyang Technological University, 50 Nanyang Avenue, Singapore 639798, Singapore*

(Received 5 October 2007; accepted 16 April 2008; published online 6 May 2008)

A "misfit strain-temperature" phase diagram for $BiFeO_3$ thin film was constructed based on the Landau–Devonshire theory with the mechanical substrate effect. It is found that the polarization instabilities result in the formation of the monoclinic phases in $BiFeO_3$ thin films. The effective substrate lattice parameter has been introduced to calculate the film thickness dependence of the polarization and the dielectric constants. The theoretical results are in agreement with the experimental data for the thickness dependence of ferroelectric properties of the $BiFeO_3$ epitaxial thin films on $SrTiO_3$ and Si substrates. © *2008 American Institute of Physics*.
[DOI: 10.1063/1.2920192]

Multiferroic materials have recently attracted great attention in the development of multifunctional materials. One of the key materials is the $BiFeO_3$ (BFO), which possesses the coexistence of ferroelectric and antiferromagnetic order and is characterized by the ferroelectric Curie temperature $T_C \sim 830\,^\circ C$ and antiferromagnetic Néel temperature $T_N \sim 370\,^\circ C$.[1,2] The bulk BFO single crystal has been shown to possess a rhombohedra perovskite structure ($a=b=c=5.63$ Å, $\alpha=\beta=\gamma=59.4°$) at room temperature, which belongs to the space group $R3c$.[3,4] The spontaneous polarization $P_s$ of the single crystal is oriented along the $[111]_c$ direction at 77 K with a value of 6.1 $\mu C/cm^2$.[5] Much larger ferroelectric polarizations have been reported in epitaxial thin films of BFO.[6,7] The remnant polarization of 50–60 $\mu C/cm^2$ was measured in the 200-nm-thick BFO thin film grown by pulsed laser deposition onto the $(100)_c$ single crystal $SrTiO_3$ (STO) substrate.[6] A 200-nm-thick BFO thin film on Si substrate with STO as a template layer was characterized by the remnant polarization of about 45 $\mu C/cm^2$.[7] Moreover, the phase-pure 200-nm-thick BFO films oriented along the $(001)_c$, $(110)_c$, and $(111)_c$ directions have the remnant polarizations of 55, 80, and 100 $\mu C/cm^2$, respectively, with the conducting perovskite oxide bottom electrodes $SrRuO_3$ (SRO) on STO substrate.[8] Recently, a monoclinic structure in the epitaxial BFO thin film deposited on DyScO3 substrate was reported as well.[9]

For epitaxial systems, the substrate-induced strains have been proven to have great influence on the ferroelectric properties of ferroelectric materials.[10–12] The dependence of physical properties on misfit strain was carried out by using Landau–Devenshire (LD) phenomenological theory.[13,14] It was shown that the appearance of unusual phases and phase transformations result from the epitaxial-induced internal stresses.[14] Based on an assumption of a tetragonal BFO thin film structure, the film thickness effect was described for BFO thin film grown on the $(001)_c$-oriented STO substrate.[15] Another recent report described the effects of various substrate-induced strains on the spontaneous polarizations of BFO, mainly on strain and orientation effects.[16]

In this letter, misfit strain-temperature phase diagrams were developed to describe the film thickness dependence of ferroelectric properties for the epitaxial $(001)_c$ BFO films, using the frame of LD model with consideration of the effect of film thickness.[14,17] In the calculations, we did not include the magnetic effect and the coupling between magnetic order and ferroelectric orders at the first step, owing to a relative weak magnetic order compared to a stronger ferroelectric one. In constructing the misfit strain-temperature phase diagram for BFO thin film, we consider that a single domain $(001)_c$ BFO film epitaxially grows in the cubic paraelectric phase on the thick cubic substrate under short-circuit electrical boundary conditions. The thermodynamic potential of pseudocubic BFO film is expressed as the function of polarization $P_i(i=1,2,3)$, temperature $T$, misfit strain $u_m=(a_s-a_f)/a_s$, where $a_s$ is the in-plane lattice parameter for substrate and $a_f$ is the equivalent cubic lattice constant of the free standing film. The expression of thermodynamic potential follows,[14,17]

$$\tilde{G} = a_1^*(P_1^2+P_2^2)+a_3^*P_3^2+a_{11}^*(P_1^4+P_2^4)+a_{33}^*P_3^4 + a_{13}^*(P_1^2P_3^2+P_2^2P_3^2)+a_{12}^*P_1^2P_2^2+\frac{u_m^2}{S_{11}+S_{22}}, \quad (1)$$

with the following renormalized coefficients of the free energy expansion:

$$a_1^* = a_1 - u_m\frac{Q_{11}+Q_{12}}{S_{11}+S_{12}}, \quad a_3^* = a_1 - u_m\frac{2Q_{12}}{S_{11}+S_{12}},$$

$$a_{11}^* = a_{11}+\frac{1}{2}\frac{1}{S_{11}^2-S_{12}^2}[(Q_{11}^2+Q_{12}^2)S_{11}-2Q_{11}Q_{12}S_{12}],$$

$$a_{33}^* = a_{11}+\frac{Q_{12}^2}{S_{11}+S_{12}},$$

$$a_{12}^* = a_{12}-\frac{1}{S_{11}^2-S_{12}^2}[(Q_{11}^2+Q_{12}^2)S_{11}-2Q_{11}Q_{12}S_{12}] + \frac{Q_{44}^2}{2S_{44}},$$

[a]Electronic mail: langchen@ntu.edu.sg.

 

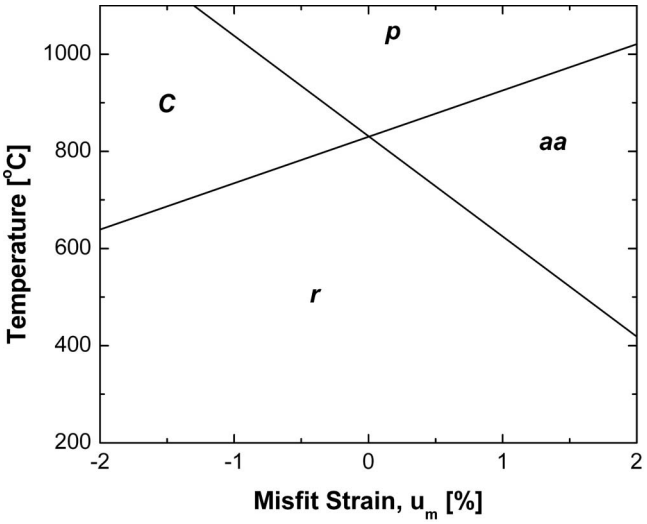


FIG. 1. Misfit-temperature phase diagram of a $(001)_c$ single-domain BFO thin film grown on a cubic substrate.

$$a_{13}^{*} = a_{12} + \frac{Q_{12}(Q_{11}+Q_{12})}{S_{11}+S_{12}}, \tag{2}$$

where $a_1$ is the dielectric stiffness, $a_{ij}$ and $a_{ijk}$ are the higher order stiffness coefficients at constant stress, $Q_{ij}$ are the electrostrictive coefficients, and $S_{ij}$ are the elastic compliances of the film. $a_1=(T-T_0)/2\varepsilon_0 C$, where $T_0$ and $C$ are Curie–Weiss temperature and constant of a bulk ferroelectric, and $\varepsilon_0$ is the permittivity of the free space. Only $a_1$ is temperature dependent and the other parameters are temperature independent. Due to the lack of sufficient experimental data to obtain the reliable values of all higher order coefficients especially that for the sixth-order terms, the LG potential of Eq. (1) used expansions only to the fourth order. The parameters and coefficients used for computation are mainly obtained by referring to the previous data published.[16,18] The theoretical results predicted by calculation are still in agreement with the experimental ones as shown below.

Six phases in the numerical calculation were considered: (i) *paraelectric* phase, where $P_1=P_2=P_3=0$; (ii) the ***c*** phase, where $P_1=P_2=0$ and $P_3\neq 0$; (iii) the ***a*** phase, where $P_1\neq 0$, and $P_2=P_3=0$; (iv) the ***ac*** phase, where $P_1\neq 0, P_2=0$, and $P_3\neq 0$; (v) the ***aa*** phase, where $P_1=P_2\neq 0$ and $P_3=0$; and (vi) the ***r*** phase, where $P_1=P_2\neq 0$ and $P_3\neq 0$. All of the minima of $\tilde{G}(u_{m,}, P_i, T)$ with respect to the components of the polarization were calculated, and the phase with the minimum free energy was selected as the stable phase shown in Fig. 1.

There are some distinct features of the phase diagrams as follows. (1) According to Fig. 1, the paraelectric phase, the ***c*** phase, the ***r*** phase, and the ***aa*** phase appear in the examined temperature and misfit strain range. The appearance of ***aa*** phase (with in-plane polarization) results from the positive misfit (i.e., tensile stress), while the ***c*** phase with the polarization vector perpendicular to the film/substrate interface results from the negative misfit strain (i.e., compressive stress). (2) Since the ***r*** phase is characterized by monoclinic structure in the wide rage, the appearance of the ***r*** phase is consistent with the experimental observations that the compressive strain from the STO substrate reduces the rhombohedral symmetry $R3c$ of bulk BFO to monoclinic structure for BFO films grown on STO, Si, and $DyScO_3$ substrates.[9,19,20](3) It is shown from Fig. 1 that the misfit strain will result in the change in Curie temperature, where the paraelectric state turns into a ferroelectric state. The Curie temperature will increase whether the misfit strain is positive or negative. Moreover, the positive sign of the coefficients $a_{ij}^{*}$ indicates the second order phase transition in the constrained BFO films. (4) The ***r*** phase is characterized by the components along all the three crystal axes ($P_1=P_2\neq 0$ and $P_3\neq 0$), the angle $\Psi$ between the spontaneous polarization $P_s$ ($P_s=\sqrt{2P_1^2+P_3^2}$), and the polarization along the $[001]_c$ will change as the function of the misfit strain at the room temperature (RT=25 °C). The angle changes from 35° to 45° in the misfit strain range [−1.0%, 1.0%] as shown in Fig. 2, which indicates that the existence of monoclinic phases is due to the distortion of a rhombohedral parent phase.

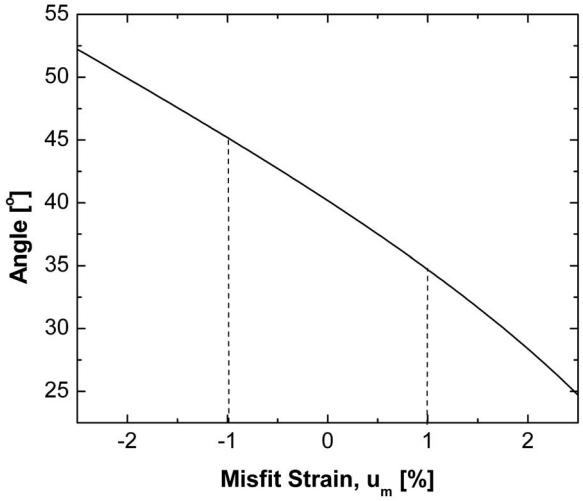


FIG. 2. Angle $\Psi$ between the spontaneous polarization $P_s$ ($Ps=\sqrt{2P_1^2+P_3^2}$) and the polarization along $[001]_c$ will change as the function of the misfit strain at the room temperature (RT=25 °C).

The effective substrate lattice parameter has been introduced to describe the film thickness dependence of epitaxial misfit strain due to relaxation by misfit dislocations during film deposition.[15,17] The effective substrate lattice $\tilde{a}_s$ is de-

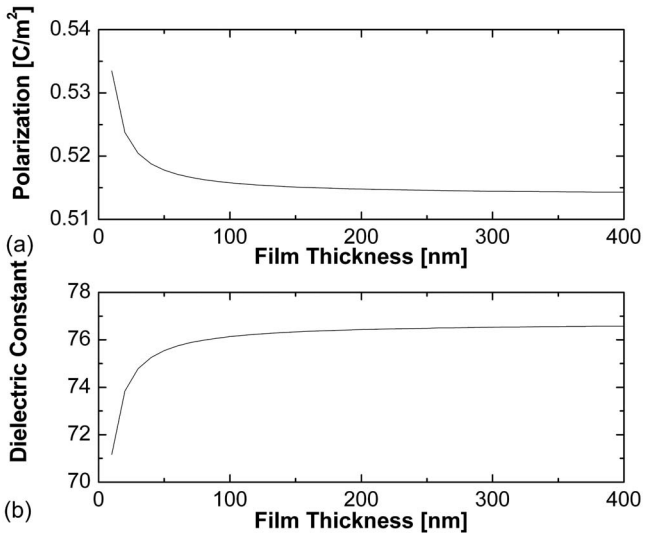


FIG. 3. Theoretical results of film thickness dependence of (a) spontaneous polarization and (b) relative dielectric constants of an epitaxial BFO thin film on a STO substrate.

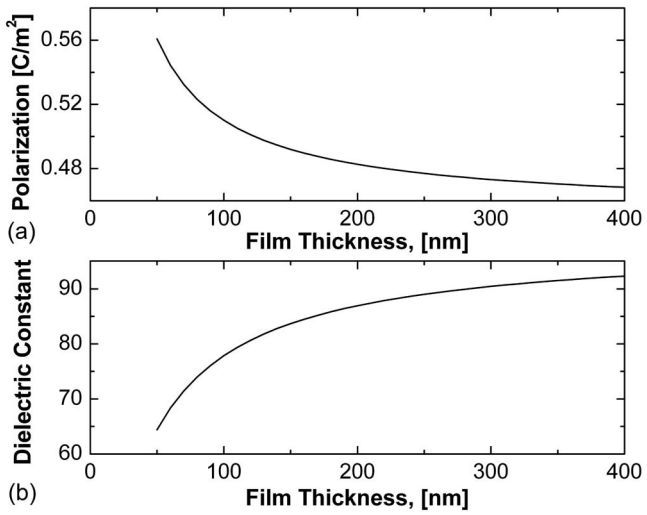


FIG. 4. Theoretical results of film thickness dependence of (a) spontaneous polarization and (b) relative dielectric constants of an epitaxial BFO thin film on a Si substrate.

fined as $\tilde{a}_s = a_s(T)/\rho a_s(T) + 1$, where $\rho$ is the equilibrium linear misfit dislocation density at the deposition temperature $T_G$. $\rho = u_m(T_G)/a_s(T_G)(1 - h_\rho/h)$, where $h_\rho$ is the critical film thickness corresponding to the generation of the misfit dislocation, and $u_m(T_G)$ and $a_s(T_G)$ are the misfit strain and lattice constant of substrate at the deposition temperature $T_G$. Moreover, the lattice parameters at $T_G$ can be obtained by the lattice parameters at RT and the thermal expansion coefficients (TEC). We consider the ferroelectric properties of $BiFeO_3$ epitaxial thin films grown on both Si substrate and $SrTiO_3$ substrate at room temperature. For both cases, the lattice constant for BFO thin film is 3.96 Å at RT and the TEC $= 10.0 \times 10^{-6}$ K$^{-1}$ for BFO thin film.[7,21,22] We take $a_s = 3.82$ Å, $h_\rho = 25$ nm, and TEC $= 3.0 \times 10^{-6}$ K$^{-1}$ for Si substrate, and $a_s = 3.91$ Å, $h_\rho = 10$ nm with TEC $= 11.7 \times 10^{-6}$ K$^{-1}$ for $SrTiO_3$ substrate.[7,22]

The dependence of the spontaneous polarization $P_0$ with respect to the film thickness is illustrated in Figs. 2(a) and 3(a). It has shown that the spontaneous polarization increases as the film thickness decreases and this result is consistent with the experimental results. Since experimental *P-E* curve is close to square,[15] the value of spontaneous polarization $P_0$ has been used to compare to the experimental data of remnant polarization. The $P_0$ of 200-nm-thick on Si substrate is $\sim 47\ \mu C/cm^2$, which agrees with the experimental value of 45 $\mu C/cm^2$; $P_0$ of 200-nm-thick on STO substrate is $\sim 52\ \mu C/cm^2$, which is also consistent with the experimental value of 55 $\mu C/cm^2$. The expression for relative dielectric constant of ***r*** phase is given as $\varepsilon_{33}/\varepsilon_0 = 1/2\varepsilon_0(a_3^* + 2a_{13}^* P_{r1}^2 + 6a_{33}^* P_{r3}^2)$ in Figs. 2(b) and 3(b), where $P_1^2 = P_2^2 = P_{r1}^2 = a_{13}^* a_3^* - 2a_1^* a_3^*/4a_{11}^* a_{33}^* + 2a_{12}^* a_{33}^* - 2a_{13}^{*2}$, $P_3^2 = P_{r3}^2 = 2a_{13}^* a_1^* - 2a_{11}^* a_3^* - a_{12}^* a_3^*/4a_{11}^* a_{33}^* + 2a_{12}^* a_{33}^* - 2a_{13}^{*2}$, and the subscript *r* refers to **r** phase.[17] The dielectric constants by the simulation will increase with the film thickness in Figs. 2(b) and 3(b), and the trend is consistent with the experimental data.[23] The dielectric constant (at the 200 nm thickness) for the STO substrate is about 80, while the experiment data is 100.[23] The dielectric constant (at the 400 nm thickness) for the Si substrate is close to 95 (see Fig. 4), while the experimental one is 120.[24] The theoretical results of dielectric constant cannot recover all the experimental ones and one reason for this is due to other extrinsic effects such as domain structures in BFO thin films.

In summary, we have studied the substrate-induced strain on phase transition of the single-domain epitaxial BFO film with the consideration of thin film thickness effect. The misfit strain-temperature phase diagram for BFO thin film has been built on the basis of a LD phenomenological frame and the appearance of **r** phase in the phase diagram agrees well with experimental data, especially for the polarizations of BFO films on STO and Si substrates.

We acknowledge the financial support from Nanyang Technological University under Grant SUG 06-13, NTU-TL seed fund and Grant RG21/07.

[1] V. A. Murashav, D. N. Rakov, V. M. Ionov, L. S. Dubenko, and Y. U. Titov, Ferroelectrics **162**, 11 (1994).
[2] Yu. F. Popov, A. M. Kadomtseva, G. P. Vorobev, and A. K. Zvezdin, Ferroelectrics **162**, 135 (1994).
[3] A. G. Tutov, Fiz. Tverd. Tela (S.-Peterburg) **11**, 2681 (1969).
[4] G. D. Achenbach, R. Gerson, and W. J. James, J. Am. Ceram. Soc. **50**, 437 (1967).
[5] J. R. Teague, R. Gerson, and W. J. James, Solid State Commun. **8**, 1073 (1970).
[6] J. Wang, J. B. Neaton, H. Zheng, V. Nagarajan, S. B. Ogale, B. Liu, D. Viehland, V. Vaithyanathan, D. G. Schlom, U. V. Waghmare, N. A. Spaldin, K. M. Rabe, M. Wuttig, and R. Ramesh, Science **299**, 1719 (2003).
[7] J. Wang, H. Zheng, Z. Ma, S. Prasertchough, M. Wuttig, R. Droopad, J. Yu, K. Eisenbeiser, and R. Ramesh, Appl. Phys. Lett. **85**, 2574 (2004).
[8] J. F. Li, J. Wang, M. Wuttig, R. Ramesh, N. Wang, B. Ruette, A. P. Pyatakov, A. K. Zvezdin, and D. Viehland, Appl. Phys. Lett. **84**, 5261 (2004).
[9] Y. H. Chu, T. Zhao, M. P. Cruz, Q. Zhan, P. L. Yang, L. W. Martin, M. Huijben, C. H. Yang, F. Zavaliche, H. Zheng, and R. Ramesh, Appl. Phys. Lett. **90**, 252906 (2007).
[10] K. J. Choi, M. Biegalski, Y. L. Li, A. Sharan, J. Schubert, R. Reiche, Y. B. Chen, X. Q. Pan, V. Gopalan, L. Q. Chen, D. G. Schlom, and C. B. Eom, Science **306**, 1005 (2004).
[11] J. H. Haeni, P. Irvin, W. Chang, P. Vecker, P. Reiche, Y. L. Li, S. Chaoudhury, W. Tian, M. E. Hawley, B. Creigo, A. K. Tagantsev, X. Q. Pan, and S. K. Streiffer, Nature (London) **30**, 758 (2004).
[12] F. Tsui, M. C. Smoak, T. K. Nath, and C. B. Eom, Appl. Phys. Lett. **76**, 2421 (2000).
[13] W. Chang, C. M. Gilmore, W. J. Kim, J. M. Pond, S. W. Kirchoefer, S. B. Qadri, D. B. Chrisey, and J. S. Horwitz, J. Appl. Phys. **87**, 3044 (2004).
[14] N. A. Pertsev, A. G. Zembilgotov, and A. K. Tagantsev, Phys. Rev. Lett. **80**, 1988 (1998).
[15] Q. Jiang and J. H. Qiu, J. Appl. Phys. **99**, 103901 (2006).
[16] J. X. Zhang, Y. L. Li, Y. Wang, Z. K. Liu, L. Q. Chen, Y. H. Chu, F. Zavaliche, and R. Ramesh, J. Appl. Phys. **101**, 114105 (2007).
[17] Z. G. Ban and S. P. Alpay, J. Appl. Phys. **91**, 9288 (2002).
[18] The list of the parameters of $G$ (in SI units, the temperature $T$ in °C) used in the calculation: $a_1 = 4.9 \times (T - 830) \times 10^5$; $a_{11} = 6.5 \times 10^8$; $a_{12} = 1.0 \times 10^8$; $S_{11} = 6.3 \times 10^{-12}$; $S_{12} = -0.85 \times 10^{-12}$; $Q_{11} = 0.032$; $Q_{12} = -0.016$; $Q_{44} = 0.01$; and $S_{44} = 1.47 \times 10^{-11}$.
[19] G. Xu, H. Hiraka, G. Shirane, J. F. Li, J. Wang, and D. Viehland, Appl. Phys. Lett. **86**, 182905 (2005).
[20] G. Xu, J. Li, and D. Viehland, Appl. Phys. Lett. **89**, 222901 (2006).
[21] X. Qi, M. Wei, Y. Lin, Q. Jia, D. Zhi, J. Dho, G. B. Mark, and L. M. Judith, Appl. Phys. Lett. **86**, 071913 (2005).
[22] B. S. Kwak, A. Erbil, J. D. Budai, M. F. Chisholm, L. A. Boatner, and B. J. Wilkens, Phys. Rev. B **49**, 14865 1994.
[23] J. Wang, Ph.D. thesis, University of Maryland, 2005.
[24] S. K. Singh, H. Ishiwara, and K. Maruyama, J. Appl. Phys. **100**, 064102 (2006).